Potentials versus Geometry, Revisited*

T. Curtright[§] and S. Subedi[∞]

Department of Physics, University of Miami, Coral Gables, Florida 33124

[§]curtright@miami.edu [∞]sushil.subedi04@gmail.com

Abstract

We revisit an old subject to discuss relationships between the dynamics for particles subjected to potentials and the dynamics for particles moving freely on background geometries, in the context of non-relativistic quantum mechanics. In particular, we illustrate how selected geometries can be used to regularize singular potentials. We also compute scattering amplitudes for quanta incident on a static non-relativistic wormhole.

Contents

1 Introduction

Given a solution to Einstein's theory of gravity acting as a background spacetime geometry, it is well-known that particle motion on this fixed geometry can be described by an effective potential [1]. But given a potential, it is perhaps less widely recognized that an equivalent particle dynamics can be described by an effective geometry. This equivalence is discussed here in the context of non-relativistic quantum mechanics. That is to say, only the non-relativistic form of Schrödinger's equation is used in our discussion, and only spatial dimensions are allowed non-trivial geometry, while time is taken to be common to all frames and universal to all observers.

Geometrical models can be related to potential models in ways that often make the physics easier to extract and understand from the perspective of one or the other side of the relationship. For a generic potential the corresponding geometry can be singular, especially if the potential is singular (e.g. inverse powers of r). On the other hand, non-singular geometries can give regularized forms of singular potentials that specify the essential physical features of those potentials without mathematical ambiguities or pathologies.

*Not quite the same as *Ford v Ferrari*. Or is it?

2 Non-relativistic Theory

Consider a non-relativistic particle of mass μ with energy $E = \hbar^2\varepsilon/(2\mu)$, subject to a potential $V(\overrightarrow{r}) = \hbar^2 U(\overrightarrow{r})/(2\mu)$, and whose wave function is a solution of the Schrödinger equation in flat Euclidean space.

$$-\nabla^2\Psi + U\Psi = \varepsilon\Psi \tag{1}$$

Equivalence between this potential problem and a suitably chosen non-flat geometry can be obtained by relating the solutions of (1) with those for *free* particle motion on a specified manifold, written as

$$-\frac{1}{\sqrt{g}}\partial_\mu\left(\sqrt{g}g^{\mu\nu}\partial_\nu\Psi\right) = \varepsilon\Psi \tag{2}$$

In particular, given a rotationally invariant potential, $U(r)$, for a particle with specified angular momentum there is an equivalent radial Schrödinger equation that describes a particle moving freely on a curved space whose geometry is nontrivial, and vice versa. The main result can be expressed in general as an integro-differential modification of the Riccati equation [2].

In the case of two spatial dimensions (2D) with Euclidean signature, for a particle with angular momentum m so that the particle's wave function factorizes as $\Psi(r,\theta) = \Psi_m(r)\exp(im\theta)$, the main result is

$$\frac{dW}{dr} + W^2 + \frac{m^2}{R_0^2}\exp\left(-4\int_{r_0}^{r} W(\mathfrak{r})\,d\mathfrak{r}\right) = U(r) + \frac{m^2 - 1/4}{r^2} \tag{3}$$

Upon solving (3), the function W encodes the geometry in terms of the invariant distance on the curved 2D space as

$$(ds)^2 = (dr)^2 + R^2(r)(d\theta)^2 \quad \text{with} \quad R(r) = R_0\exp\left(2\int_{r_0}^{r} W(\mathfrak{r})\,d\mathfrak{r}\right) \quad \text{i.e.} \quad W(r) = \frac{d}{dr}\ln\sqrt{R(r)} \tag{4}$$

and the invariant Laplacian on the 2-manifold is

$$\frac{1}{\sqrt{g}}\partial_\mu\left(\sqrt{g}g^{\mu\nu}\partial_\nu\right) = \frac{1}{R(r)}\partial_r\left(R(r)\,\partial_r\right) + \frac{1}{R(r)^2}\partial_\theta^2 = \partial_r^2 + 2W(r)\,\partial_r + \frac{1}{R(r)^2}\partial_\theta^2 \tag{5}$$

Alternatively, given the geometry of the surface with a specified $R(r)$, the corresponding effective potential in flat space for angular momentum m is given by

$$U(r) = \frac{1}{2}\frac{R''(r)}{R(r)} - \frac{1}{4}\left(\frac{R'(r)}{R(r)}\right)^2 + \left(\frac{m}{R(r)}\right)^2 - \frac{m^2 - \frac{1}{4}}{r^2} \tag{6}$$

As should be expected, for $R(r) \neq r$ this effective radial potential will depend on the angular momentum.

To establish the relation between the potential problem in 2D flat space and the 2D curved space system without a potential, it is only necessary to eliminate the first derivative term in (5) by writing $\Psi(r,\theta) = \exp\left(-\int_{r_0}^{r} W(\mathfrak{r})\,d\mathfrak{r}\right)\psi(r,\theta)$ to obtain

$$\left(\partial_r^2 + 2W(r)\,\partial_r + \frac{1}{R(r)^2}\partial_\theta^2\right)\Psi(r,\theta) = \exp\left(-\int_{r_0}^{r} W(\mathfrak{r})\,d\mathfrak{r}\right)\left(\partial_r^2 + \frac{1}{R(r)^2}\partial_\theta^2 - W' - W^2\right)\psi(r,\theta) \tag{7}$$

and compare this to the flat space system with a potential U, as obtained by writing $\Psi(r,\theta) = \psi(r,\theta)/\sqrt{r}$, namely,

$$\left(\partial_r^2 + \frac{1}{r}\partial_r + \frac{1}{r^2}\partial_\theta^2 - U(r)\right)\Psi(r,\theta) = \frac{1}{\sqrt{r}}\left(\partial_r^2 + \frac{1}{r^2}\partial_\theta^2 - U(r) + \frac{1}{4r^2}\right)\psi(r,\theta) \tag{8}$$

Separating variables as $\psi(r,\theta) = \psi_m(r)\exp(im\theta)$ for both (7) and (8) leads to the same second-order radial equation provided

$$-\frac{m^2}{R(r)^2} - W' - W^2 = -\frac{\left(m^2 - 1/4\right)}{r^2} - U(r) \tag{9}$$

and hence (3) with $R(r) = R_0 \exp\left(2\int_{r_0}^{r} W(\mathfrak{r})\, d\mathfrak{r}\right)$, or alternatively (6).

In the case of N spatial dimensions (ND) with Euclidean signature [3], on a manifold with isotropic metric of the same form as (4), a particle with angular momentum ℓ has a wave function that factorizes as $\Psi = \Psi_\ell(r)\, Y_{\ell m_1 m_2 \cdots m_{N-2}}(\Omega)$, with all the angular dependence in the hyperspherical harmonics $Y_{\ell m_1 m_2 \cdots m_{N-2}}(\Omega)$. The invariant Laplacian acting on Ψ is

$$\frac{1}{\sqrt{g}}\partial_\mu\left(\sqrt{g}g^{\mu\nu}\partial_\nu\right)\Psi = \frac{1}{R(r)^{N-1}}\,\partial_r\left(R(r)^{N-1}\,\partial_r\right)\Psi - \frac{1}{R(r)^2}\,L^2\Psi \tag{10}$$

where all the $N-1$ angular derivatives are contained in $L_{jk} \equiv -i\left(x_j\partial_k - x_k\partial_j\right)$ with $L^2 \equiv \sum_{1\le j<k\le N} L_{jk}L_{jk}$. The $Y_{\ell m_1 m_2 \cdots m_{N-2}}$ are eigenfunctions of L^2 and form a complete set on the hypersphere, S_{N-1}, analogous to the familiar spherical harmonics $Y_{\ell m}$ on S_2. Acting on $Y_{\ell m_1 m_2 \cdots m_{N-2}}$ the L^2 eigenvalues are given by [4]

$$L^2 Y_{\ell m_1 m_2 \cdots m_{N-2}} = \ell(\ell+N-2)\, Y_{\ell m_1 m_2 \cdots m_{N-2}} \tag{11}$$

for $\ell = 0, 1, 2, \cdots$, generalizing the well-known $N = 3$ case. The eigenvalue equation (2) then reduces to the radial equation

$$\frac{-1}{R(r)^{N-1}}\,\partial_r\left(R(r)^{N-1}\,\partial_r\Psi_\ell(r)\right) + \frac{\ell(\ell+N-2)}{R(r)^2}\Psi_\ell(r) = \varepsilon\Psi_\ell(r) \quad \text{for} \quad 0 \le r \le \infty \tag{12}$$

Comparison to a potential system in ND flat space, (1), again leads to the main result in the form of a modified Riccati equation.

$$\frac{dW}{dr} + W^2 + \frac{\ell(\ell+N-2)}{R_0^2}\,\exp\left(\frac{4}{1-N}\int_{r_0}^{r} W(\mathfrak{r})\, d\mathfrak{r}\right) = U(r) + \frac{\left(\ell+\frac{1}{2}(N-1)\right)\left(\ell+\frac{1}{2}(N-3)\right)}{r^2} \tag{13}$$

Upon solving for the function W, the effective geometry is encoded in the invariant distance on the curved ND space as

$$(ds)^2 = (dr)^2 + R^2(r)\,(d\Omega)^2 \quad \text{with} \quad R(r) = R_0\exp\left(\frac{2}{N-1}\int_{r_0}^{r} W(\mathfrak{r})\, d\mathfrak{r}\right) \quad \text{i.e.} \quad W(r) = \frac{N-1}{2}\frac{d}{dr}\ln R(r) \tag{14}$$

Alternatively, given the geometry of the surface with a specified $R(r)$, the corresponding potential in flat space for angular momentum ℓ is given by

$$U(r) = \frac{(N-1)}{2}\frac{d^2}{dr^2}\ln R(r) + \left(\frac{N-1}{2}\right)^2\left(\frac{d}{dr}\ln R(r)\right)^2 + \frac{\ell(\ell+N-2)}{R^2(r)} - \frac{\left(\ell+\frac{1}{2}(N-1)\right)\left(\ell+\frac{1}{2}(N-3)\right)}{r^2} \tag{15}$$

As in the 2D case, for $R(r) \neq r$ this effective radial potential will depend on the angular momentum.

3 Examples

For $\ell = 0$ "s-wave" solutions, (13) is an *unmodified* Riccati equation, a first-order differential equation whose solutions are well-studied [2]. For a $1/r$ potential in ND, *plus a constant*, the $\ell = 0$ case alone provides an illustration of potential $\Longrightarrow$ effective geometry. Let

$$U(r) = \frac{\kappa}{r} + \frac{\kappa^2}{(N-1)^2} \tag{16}$$

so that (13) for $\ell = 0$ becomes

$$\frac{dW}{dr} + W^2 = \frac{\kappa}{r} + \frac{\kappa^2}{(N-1)^2} + \frac{(N-1)(N-3)}{4r^2} \tag{17}$$

A particularly simple, rational solution is immediately seen to be

$$W(r) = \frac{N-1}{2r} + \frac{\kappa}{N-1} \tag{18}$$

with general solutions obtained by quadrature [2].

The 3D case is exceptional in that there is no $1/r^2$ term on the RHS of the Riccati equation when $\ell = 0$. This physically interesting case readily admits another solution for a pure Coulomb potential, sans constant, namely,[1]

$$\begin{aligned} \frac{dW(r)}{dr} + W^2(r) &= \frac{\kappa}{r} \quad \text{for} \quad N = 3 \quad \text{with} \\ W(r) = \sqrt{\frac{\kappa}{r}} \frac{I_0\left(2\sqrt{\kappa r}\right)}{I_1\left(2\sqrt{\kappa r}\right)} &= \frac{1}{r} + \frac{\kappa}{2} - \frac{\kappa^2 r}{12} + O\left(r^2\right) \end{aligned} \tag{19}$$

which is well-approximated by (18) for small r. But as before, this is a solution only for $\ell = 0$.

The effective geometry corresponding to the solution (18) is given by

$$R(r) = Kre^{2\kappa r/(N-1)^2}\ , \quad K = \frac{R_0}{r_0}\ e^{-2\kappa r_0/(N-1)^2} \tag{20}$$

The invariant distance for this particular ND manifold is then

$$(ds)^2 = (dr)^2 + K^2 r^2 e^{4\kappa r/(N-1)^2} (d\Omega)^2 \tag{21}$$

In terms of more conventional isotropic coordinates, such that $(ds)^2 = \left(\frac{dr(\rho)}{d\rho}\right)^2 (d\rho)^2 + \rho^2 (d\Omega)^2$, let

$$\rho^2 = K^2 r^2 e^{4\kappa r/(N-1)^2} \tag{22}$$

and solve for $r(\rho)$ in terms of the Lambert W function. For a repulsive potential $\kappa \geq 0$, and thus

$$r(\rho) = \frac{(N-1)^2}{2\kappa}\ \text{LambertW}\left(\frac{2\kappa\rho}{K(N-1)^2}\right)\ , \quad \frac{dr(\rho)}{d\rho} = \frac{(N-1)^2}{2\kappa\rho}\left(\frac{\text{LambertW}\left(\frac{2\kappa\rho}{K(N-1)^2}\right)}{1+\text{LambertW}\left(\frac{2\kappa\rho}{K(N-1)^2}\right)}\right) \tag{23}$$

The resulting geometry is described by

$$(ds)^2 = \left(\frac{(N-1)^2}{2\kappa\rho}\frac{\text{LambertW}\left(\frac{2\kappa\rho}{K(N-1)^2}\right)}{1+\text{LambertW}\left(\frac{2\kappa\rho}{K(N-1)^2}\right)}\right)^2 (d\rho)^2 + \rho^2 (d\Omega)^2 \tag{24}$$

A canonical embedding of this N-manifold into an $N+1$ Lorentz space is given by

$$(ds)^2 = (d\rho)^2 + \rho^2 (d\Omega)^2 - c^2 (dt(\rho))^2 \tag{25}$$

with

$$c\frac{dt(\rho)}{d\rho} = \frac{\sqrt{\left(1+\text{LambertW}\left(\frac{2\kappa\rho}{K(N-1)^2}\right)\right)^2 - \left(\frac{(N-1)^2}{2\kappa\rho}\text{LambertW}\left(\frac{2\kappa\rho}{K(N-1)^2}\right)\right)^2}}{1+\text{LambertW}\left(\frac{2\kappa\rho}{K(N-1)^2}\right)} \tag{26}$$

For $\kappa \geq 0$ this is a real embedding all the way down to $\rho = 0$ if $K \geq 1$. For $K < 1$ the embedding is real only for $\rho_{\min} \leq \rho \leq \infty$ where $\rho_{\min}$ is given by the positive real root of the radicand in (26).

Graphical representations of the embedded surface and generalizations to situations where $\ell \neq 0$ are left as an exercise for the reader, as is the $\kappa < 0$ situation. But it should already be evident from the $\ell = 0$ case that a repulsive $1/r$ model is more easily understood as a potential problem than it is from the geometrical side of the relationship. Rather than pursue the quantum mechanics on the resulting ND manifold for this example, we consider next a more troublesome singular potential which can be regularized by mapping onto a well-known geometry.

[1] NB This is the $1/r$ potential expressed as it would be in supersymmetric quantum mechanics.

4 Wormholes

Consider a smooth, spatial "bridge" manifold [5] (i.e. a "wormhole" [6]) given by

$$(ds)^2 = (dw)^2 + R^2(w)(d\Omega)^2 \ , \quad -\infty \leq w \leq +\infty \tag{27}$$

where $R(w) > 0$ has an absolute minimum at $w = 0$, and behaves asymptotically as $R^2(w) \underset{w\to\pm\infty}{\sim} w^2 + O\left(1/w^2\right)$. For example, the w-form of a static Ellis metric [7] in N spatial dimensions is simply

$$R^2(w) = R_0^2 + w^2 \ , \quad -\infty \leq w \leq +\infty \tag{28}$$

The metric (27) leads to the invariant Laplacian

$$\frac{1}{\sqrt{g}}\partial_\mu\left(\sqrt{g}g^{\mu\nu}\partial_\nu\Psi\right) = \frac{1}{R(w)^{N-1}}\ \partial_w\left(R(w)^{N-1}\partial_w\right) - \frac{1}{R(w)^2}\ L^2 \tag{29}$$

where again all the $N-1$ angular derivatives are contained in L^2.

The non-relativistic Schrödinger energy eigenvalue problem for a particle moving freely on this manifold is again solved by separating variables.

$$\frac{1}{\sqrt{g}}\partial_\mu\left(\sqrt{g}g^{\mu\nu}\partial_\nu\Psi\right) + \varepsilon\Psi = 0 \ , \quad \Psi = \Psi_\ell(w)\, Y_{\ell m_1 m_2\cdots m_{N-2}}(\Omega) \tag{30}$$

The effective radial equation is now

$$\frac{1}{R(w)^{N-1}}\ \partial_w\left(R(w)^{N-1}\partial_w\Psi_\ell(w)\right) + \left(\varepsilon - \frac{\ell(\ell+N-2)}{R(w)^2}\right)\Psi_\ell(w) = 0 \tag{31}$$

Rather than compare this to rotationally invariant potential scattering in ND flat space, as above, instead compare this eigenvalue equation to one-dimensional potential scattering on the line $-\infty \leq w \leq +\infty$, as given by

$$\partial_w^2\Psi_\ell(w) + (\varepsilon - U(w))\Psi_\ell(w) = 0 \tag{32}$$

To establish the sought-for relation, again just eliminate the first derivative term in (31) by writing $\Psi_\ell(w) = (R(w))^{(1-N)/2}\psi_\ell(w)$ to obtain the energy eigenvalue equation

$$\begin{aligned} 0 &= \left(\partial_w^2 + (N-1)\frac{R'}{R}\partial_w + \left(\varepsilon - \frac{\ell(\ell+N-2)}{R(w)^2}\right)\right)\Psi_\ell(w) \\ &= (R(w))^{(1-N)/2}\left(\partial_w^2 + \left(\varepsilon - \frac{1}{2}(N-1)\frac{R''}{R} - \frac{1}{4}(N-1)(N-3)\left(\frac{R'}{R}\right)^2 - \frac{\ell(\ell+N-2)}{R^2}\right)\right)\psi_\ell(w) \end{aligned} \tag{33}$$

where primes indicate derivatives with respect to w. The second-order equation (33) is the same as that for potential scattering on the line (32) if

$$U(w) = \frac{1}{2}(N-1)\frac{R''}{R} + \frac{1}{4}(N-1)(N-3)\left(\frac{R'}{R}\right)^2 + \frac{\ell(\ell+N-2)}{R^2} \tag{34}$$

4.1 Static Ellis Metric

For the Ellis metric (28), $R' = w/R$, $R'' = R_0^2/R^3$, so

$$U(w) = (N+2\ell-3)(N+2\ell-1)\frac{1}{4R(w)^2} - (N-1)(N-5)\frac{R_0^2}{4R(w)^4} \tag{35}$$

In particular, for 3D,

$$U(w) = \frac{\ell(\ell+1)}{R_0^2+w^2} + \frac{R_0^2}{(R_0^2+w^2)^2} \quad \text{for} \quad N = 3 \tag{36}$$

This $U(w)$ may be thought of as a regularized form of $1/r^4$, a singular potential that has been well-studied in 3D [8, 9].

The angular momentum *in*dependent $1/R^4$ term in the potential (35) is repulsive for $N \leq 4$, absent for $N = 5$, and attractive for $N \geq 6$. (It so happens to be a regularized form of an attractive electrostatic potential for a point particle for $N = 6$ [3, 10].) In any case, non-relativistic scattering for the regular potential $U(w)$ has both elastic and inelastic components for all $N \geq 2$, where elastic scattering is interpreted as both incident and emergent probability flux on the "upper" branch of the wormhole manifold, and inelastic scattering is to be understood as emergent flux on the "lower" branch of the manifold, without any incident flux on that lower branch. For incident flux on the wormhole's upper branch, with $R_0 > 0$, there is always some probability flow through the bridge joining the two branches so that particles are effectively absorbed by the wormhole, as viewed by an observer located on the upper branch. For any N, the time independent partial wave scattering amplitudes can be determined exactly for $U(w)$ in terms of spheroidal wave functions [11]. An Argand diagram of the phase shifts clearly reveals the inelastic behavior. This is discussed in considerable detail in [12].

The singular $1/r^4$ potential that arises from $U(w)$ in the limit as $R_0 \to 0$ is somewhat problematic, as explained in [9] and references cited therein. At issue is whether the Hamiltonian for such a potential admits a self-adjoint extension for $0 \leq r \leq \infty$, with only real eigenvalues and unitary time evolution. For a repulsive $1/r^4$ this can be arranged with an appropriate choice of boundary conditions at $r = 0$. An attractive $1/r^4$ is another story, however, with considerable ambiguity in the boundary conditions at the origin. As stated in [9]:

> "Thus the basic feature of an attractive singular potential is seen to lie in the fact that physical processes are not uniquely determined. This gives rise to the possibility of imposing unusual or unconventional boundary conditions in physical problems as a means of representing particular physical processes. An example of a process of this type is provided by particle absorption or capture."

> "Since the deficiency indices are infinite, nonself-adjoint extensions are possible which would correspond to boundary conditions which describe inelastic scattering."

> "Thus, in the singular case, the long-range part of the force between particles does not alone suffice to determine their behavior; some cutoff mechanism apparently must be provided."

The regularization defined by the wormhole geometry avoids all these ambiguities. The Hamiltonian for a non-relativistic system governed by $U(w)$ is manifestly self-adjoint for $R_0 > 0$ when defined on a rigged Hilbert space with the usual boundary conditions as $w \to \pm\infty$. But there is a price to be paid for this mathematical convenience, namely, inelastic scattering, even when the potential is repulsive. This feature for $U(w)$ is discussed further in [12]. However, examples of such inelastic behavior can also be found in a class of wormhole deformations, especially in the limit where the wormhole throat reduces to an intrinsically flat hypercylinder.

4.2 A class of deformed wormholes

An class of static wormholes may be defined in N spatial dimensions by [14, 15]

$$R(w) = \left(R_0^n + w^n\right)^{1/n} = R_0 P(x, n) \tag{37}$$

for even integer $n \geq 2$, where we have defined the wormhole "profile" using an L^n norm on the plane, $P(x, n) = \left(1 + x^n\right)^{1/n}$ with $x = w/R_0$. This leads to

$$R_0^2 U(w) = \frac{\ell(\ell + N - 2)}{P(x, n)^2} + \frac{N - 1}{4} \frac{x^{n-2}}{P(x, n)^{2n}} \left(\left(2(n-1) + (N-3)x^n\right)\right) \tag{38}$$

In particular, in 3D,

$$R_0^2 U(w)\big|_{N=3} = \frac{\ell(\ell+1)}{P(x,n)^2} + \frac{(n-1)\,x^{n-2}}{P(x,n)^{2n}} \tag{39}$$

The 3D $\ell = 0$ and $\ell = 1$ effective potentials for various n are shown in the following graphs.

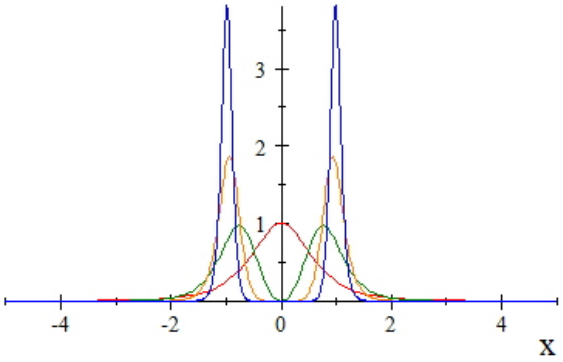

$R_0^2 U(w)\big|_{N=3,\ \ell=0}$ versus $x = w/R_0$ for $n = 2, 4, 8, 16$ in red, green, orange, and blue, respectively.

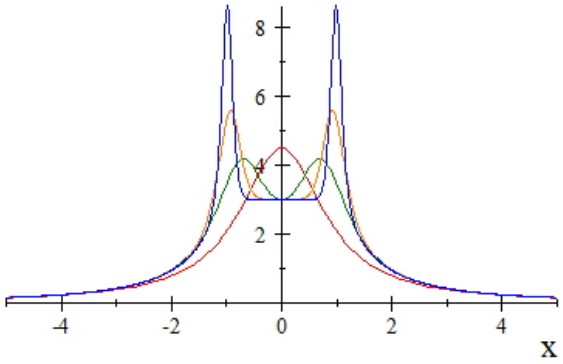

$R_0^2 U(w)\big|_{N=3,\ \ell=1}$ versus $x = w/R_0$ for $n = 2, 4, 8, 16$ in red, green, orange, and blue, respectively.

As n increases, the effective potential is similar to a δ-shell [17] but with potential spikes at *both* top and bottom edges of the wormhole. Also, in the vicinity of the wormhole's throat, for $\ell > 0$ there is a positive but *finite* effective angular momentum barrier of maximum height $\ell(\ell+1)/R_0^2$. That is to say, the asymptotic form of the $N = 3$ effective potential for the equivalent particle on the line $-\infty < x < +\infty$, as $n \to \infty$, is

$$U_\infty = \frac{\ell(\ell+1)}{R_0^2}\left(\Theta\left(1-x^2\right) + \frac{\Theta\left(x^2-1\right)}{x^2}\right) + \frac{1}{R_0^2}\left(\delta(x-1) + \delta(x+1)\right) \tag{40}$$

where $x = w/R_0$, Θ is the Heaviside step function, and δ is a Dirac delta. The finite part of $R_0^2 U_\infty$ has a simple "Devil's Tower" profile, with height $\ell(\ell+1)$.

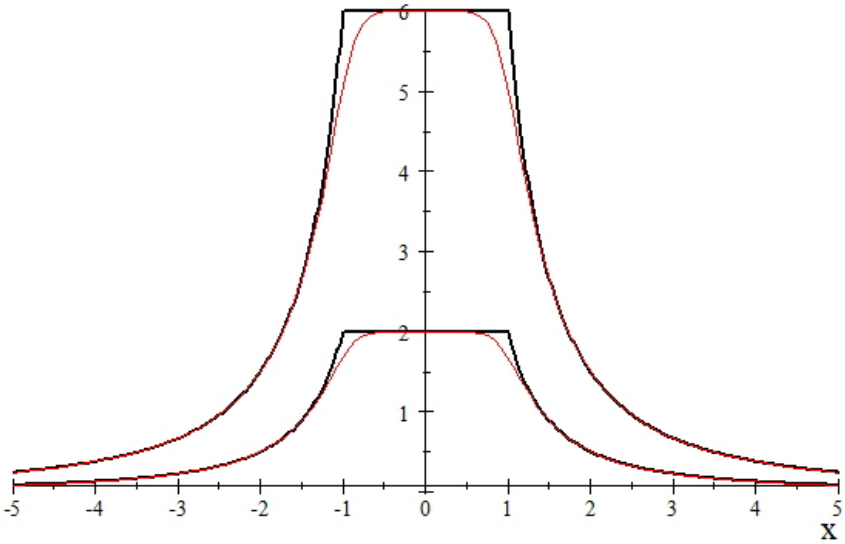

$\ell(\ell+1)\left(\Theta\left(1-x^2\right) + \frac{1}{x^2}\,\Theta\left(x^2-1\right)\right)$ for $\ell = 1, 2$, in black, compared to $\left.\frac{\ell(\ell+1)}{P(x,n)^2}\right|_{n=8}$ in red.

At first sight the Dirac deltas appearing in U_∞ might be surprising, since the invariant Laplacian only involves first derivatives of a finite continuous metric, even as $n \to \infty$, hence at most step functions due to

those first derivatives. But second derivatives of $R(w)$ occur from the Laplacian acting on the prefactor in $\Psi_\ell(w) = (R(w))^{(1-N)/2}\psi_\ell(w)$. That is to say, $R(w)''$ gives Dirac deltas as $n \to \infty$ since in that limit the manifold has infinite curvature at $w/R_0 = \pm 1$. So indeed, as $n \to \infty$ there are Dirac deltas in the unique energy eigenvalue equation for ψ_ℓ, namely, $0 = \left(\partial_w^2 + (\varepsilon - U_\infty)\right)\psi_\ell(w)$, but there are only finite terms in the corresponding eigenvalue equation for $\Psi_\ell(w)$ in that limit, albeit now the differential equation for Ψ_ℓ must be expressed piecewise. Thus $\lim_{n\to\infty} P(x,n) = 1$ if $x^2 < 1$ and $\lim_{n\to\infty} P(x,n) = |x|$ if $x^2 > 1$ leads to

$$\lim_{n\to\infty} \frac{1}{R(w)^{N-1}}\,\partial_w\left(R(w)^{N-1}\,\partial_w\Psi_\ell(w)\right) = \begin{cases} \partial_w^2\Psi_\ell(w) & \text{if} \quad w^2 < R_0^2 \\ \frac{1}{w^{N-1}}\partial_w\left(w^{N-1}\partial_w\Psi_\ell(w)\right) & \text{if} \quad w^2 > R_0^2 \end{cases} \tag{41}$$

and therefore

$$\begin{aligned} &\lim_{n\to\infty} \frac{1}{R(w)^{N-1}}\,\partial_w\left(R(w)^{N-1}\,\partial_w\Psi_\ell(w)\right) + \left(\varepsilon - \frac{\ell(\ell+N-2)}{R(w)^2}\right)\Psi_\ell(w) \\ &= \begin{cases} \partial_w^2\Psi_\ell(w) + \left(\varepsilon - \frac{\ell(\ell+N-2)}{R_0^2}\right)\Psi_\ell(w) & \text{if} \quad w^2 < R_0^2 \\ \frac{1}{w^{N-1}}\partial_w\left(w^{N-1}\partial_w\Psi_\ell(w)\right) + \left(\varepsilon - \frac{\ell(\ell+N-2)}{w^2}\right)\Psi_\ell(w) & \text{if} \quad w^2 > R_0^2 \end{cases} \end{aligned} \tag{42}$$

Nevertheless, even in the infinite n limit the solution of either eigenvalue equation leads to exactly the same results, upon realizing that

$$\lim_{n\to\infty}\Psi_\ell(w) = \begin{cases} R_0^{(1-N)/2}\psi_\ell(w) & \text{if} \quad w^2 < R_0^2 \\ w^{(1-N)/2}\psi_\ell(w) & \text{if} \quad w^2 > R_0^2 \end{cases} \tag{43}$$

More explicitly for $N = 3$, while a potential with a unit strength Dirac delta $\delta(x-1)$ implies a discontinuity in ψ' at $x = 1$, there is no such discontinuity in the derivative of $\Psi(x) = \psi(x)\,\Theta(1-x) + \frac{1}{x}\,\psi(x)\,\Theta(x-1)$. Thus

$$\begin{aligned} 0 &= \lim_{\epsilon\to 0}\int_{1-\epsilon}^{1+\epsilon}\left(\delta(x-1)\,\psi(x) - \frac{d^2}{dx^2}\psi(x)\right)dx \\ &= \psi(1) - \lim_{\epsilon\to 0}\left(\psi'(1+\epsilon) - \psi'(x-\epsilon)\right) \\ &= \psi(1) - \lim_{\epsilon\to 0}\left(\frac{d}{dx}\left(x\Psi(x)\right)\Big|_{x=1+\epsilon} - \frac{d}{dx}\Psi(x)\Big|_{x=1-\epsilon}\right) \\ &= \psi(1) - \psi(1) - \lim_{\epsilon\to 0}\left(\frac{d}{dx}\Psi(x)\Big|_{x=1+\epsilon} - \frac{d}{dx}\Psi(x)\Big|_{x=1-\epsilon}\right) \end{aligned} \tag{44}$$

Hence Ψ has a continuous first derivative at $x = 1$:

$$\lim_{\epsilon\to 0}\left(\frac{d}{dx}\Psi(x)\Big|_{x=1+\epsilon} - \frac{d}{dx}\Psi(x)\Big|_{x=1-\epsilon}\right) = 0 \tag{45}$$

For the particular $N = 3$ eigenvalue equation at hand, with energy $\varepsilon = k^2$, $\Psi_\ell(w)$ is a linear combination of $h_\ell^{(1,2)}(kw)$ for $w > R_0$, while $\psi_\ell(w)$ is a linear combination of $\sqrt{kw}H_\ell^{(1,2)}(kw)$ for $w > R_0$, but both $\Psi_\ell(w)$ and $\psi_\ell(w)$ are linear combinations of $\exp(\pm i\kappa w)$ for $-R_0 < w < R_0$, where $\kappa^2 = k^2 - \ell(\ell+1)/R_0^2$.

So then, the limit $n \to \infty$ reduces to two parallel copies of flat Euclidean space, $\mathbb{E}_N$, punctured by holes of radius R_0, and connected by a flat hypercylinder whose "top" and "bottom" boundaries consist of the two holes, as shown graphically in the Appendix. Scattering on this geometry is straightforward to analyze simply by invoking the boundary conditions of both continuous Ψ and continuous normal derivative Ψ' at each of the holes. The results may be expressed analytically in terms of Gegenbauer polynomials and Bessel functions, and may be computed numerically without great effort, as demonstrated in the next section.

4.3 Wormhole scattering amplitudes

In N spatial Euclidean dimensions, $\mathbb{E}_N$, outside a localized, rotationally invariant scattering center, the time-independent, incoming, scattered, and total wave functions are given by partial wave expansions [4].

$$\Psi_{\text{in}}\left(\overrightarrow{r}\right) = \frac{2^{(N-2)/2}\Gamma\left(\frac{N-2}{2}\right)}{4\left(kr\right)^{\frac{N-2}{2}}} \sum_{\ell=0}^{\infty} i^{\ell}\left(2\ell+N-2\right) C_{\ell}^{\left(\frac{N-2}{2}\right)}\left(\cos\theta\right) \ \left(H^{(1)}_{\ell+\frac{N-2}{2}}\left(kr\right) + H^{(2)}_{\ell+\frac{N-2}{2}}\left(kr\right)\right) \tag{46}$$

$$\Psi_{\text{sc}}\left(\overrightarrow{r}\right) = \frac{2^{(N-2)/2}\Gamma\left(\frac{N-2}{2}\right)}{4\left(kr\right)^{\frac{N-2}{2}}} \sum_{\ell=0}^{\infty} i^{\ell}\left(2\ell+N-2\right) C_{\ell}^{\left(\frac{N-2}{2}\right)}\left(\cos\theta\right) \ \left(S_{\ell}-1\right) \ H^{(1)}_{\ell+\frac{N-2}{2}}\left(kr\right) \tag{47}$$

$$\Psi_{\text{total}}\left(\overrightarrow{r}\right) = \Psi_{\text{in}}\left(\overrightarrow{r}\right) + \Psi_{\text{sc}}\left(\overrightarrow{r}\right) \tag{48}$$

Here $H^{(1,2)}_{\ell+\frac{N-2}{2}}\left(kr\right) = J_{\ell+\frac{N-2}{2}}\left(kr\right) \pm iY_{\ell+\frac{N-2}{2}}\left(kr\right)$ are Bessel functions and $C_{\ell}^{\left(\frac{N-2}{2}\right)}$ are conventionally normalized, orthogonal Gegenbauer polynomials. Of course, $\Psi_{\text{in}}\left(\overrightarrow{r}\right)$ is just a series expansion for the usual plane wave expressed in spherical coordinates, $\Psi_{\text{in}}\left(\overrightarrow{r}\right) = \exp\left(ikr\cos\theta\right)$.

The differential cross-section, $d\sigma/d\Omega_N$, follows from the radial probability flux of $\Psi_{\text{sc}}\left(\overrightarrow{r}\right)$, while the integrated cross-section is $\sigma = \int \frac{d\sigma}{d\Omega_N}\, d\Omega_N$. The result for σ in N spatial dimensions is

$$\sigma = \frac{1}{\Omega_N}\left(\frac{2\pi}{k}\right)^{N-1} \sum_{\ell=0}^{\infty} \dim\left(\ell, N\right)\left|S_{\ell}-1\right|^2 \tag{49}$$

where $\dim\left(\ell, N\right)$ is the dimension of a totally symmetric, traceless, rank ℓ tensor representation of $SO\left(N\right)$, namely,

$$\dim\left(\ell, N\right) = \frac{\left(2\ell+N-2\right)}{\Gamma\left(N-1\right)} \frac{\Gamma\left(\ell+N-2\right)}{\Gamma\left(\ell+1\right)} \tag{50}$$

and Ω_N is the total "solid angle" in N spatial dimensions, i.e. the "surface area" of a unit radius hyper-sphere, namely,

$$\Omega_N = \frac{2\pi^{\frac{N}{2}}}{\Gamma\left(\frac{N}{2}\right)} \tag{51}$$

Other ways to write the pre-factor in σ are

$$\frac{1}{\Omega_N}\left(\frac{2\pi}{k}\right)^{N-1} = \frac{1}{k^{N-1}} \ \left(4\pi\right)^{\frac{N-2}{2}} \Gamma\left(\frac{N}{2}\right) = \frac{1}{2k^{N-1}} \ \Omega_{N-1} \ \Gamma\left(N-1\right) = \frac{V_{N-1}\left(R\right)}{\left(kR\right)^{N-1}} \frac{\Gamma\left(N\right)}{2} \tag{52}$$

where $V_{N-1}\left(R\right)$ is the (hyper)volume of a ball of radius R embedded in $N-1$ dimensions.

$$V_{N-1}\left(R\right) = \frac{\Omega_{N-1}R^{N-1}}{N-1} = \frac{\pi^{\frac{N-1}{2}}R^{N-1}}{\Gamma\left(\frac{N+1}{2}\right)} \tag{53}$$

Thus we obtain the dimensionless ratio

$$\frac{\sigma}{V_{N-1}\left(R\right)} = \frac{2\Gamma\left(N\right)}{\left(kR\right)^{N-1}} \sum_{\ell=0}^{\infty} \dim\left(\ell, N\right)\left|\frac{S_{\ell}-1}{2i}\right|^2 \tag{54}$$

For example, when $N=3$, $\dim\left(\ell, 3\right) = \left(2\ell+1\right)$, and $V_2\left(R\right) = \pi R^2$, i.e. the maximum area of a cross-sectional circular disk for a sphere of radius R.

Consider scattering for the $n \to \infty$ wormhole geometry described above, with an incident plane wave $\Psi_{\text{in}}\left(\overrightarrow{r}\right)$ only on the upper copy of $\mathbb{E}_N$. The corresponding "elastic" cross section σ would be measurable by a "top-side" observer with detection apparatus only in the upper copy of $\mathbb{E}_N$, while probability flux emerging on the lower copy of $\mathbb{E}_N$ would appear as an "inelastic" contribution to the cross section and not directly detected by that top-side observer.

Imposing continuity of Ψ_{total} and $d\Psi_{\text{total}}/dw$ at the top and bottom boundaries of the hypercylinder connecting the two copies of $\mathbb{E}_N$, with cylinder radius R_0 and length L_0, the partial wave scattering amplitudes for wave functions on the upper Euclidean space are then given by

$$S_\ell = -\frac{\left(\kappa^2 h_1 h_2 - k^2 h_1' h_2'\right)\sin\left(\kappa L_0\right) + k\kappa\left(h_1 h_2' + h_2 h_1'\right)\cos\left(\kappa L_0\right)}{\left(\kappa^2 h_1^2 - k^2 (h_1')^2\right)\sin\left(\kappa L_0\right) + 2k\kappa h_1 h_1' \cos\left(\kappa L_0\right)} \tag{55}$$

where the abbreviations are as follows. For $N \geq 2$,

$$h_{1,2} = \frac{1}{(kR_0)^{\frac{N-2}{2}}}\, H^{(1,2)}_{\ell+\frac{N-2}{2}}\left(kR_0\right) \ , \quad \kappa = \sqrt{k^2 - \ell\left(\ell + N - 2\right)/R_0^2} \tag{56}$$

It follows that $|S_\ell| \neq 1$ for generic values of k, so the scattering has an inelastic component as seen by the top-side observer.

For example, consider the cases $N = 2$ and 3, the former being more readily visualized as two punctured Euclidean planes joined by a right circular cylinder, as shown here for $L_0 = 2R_0$.

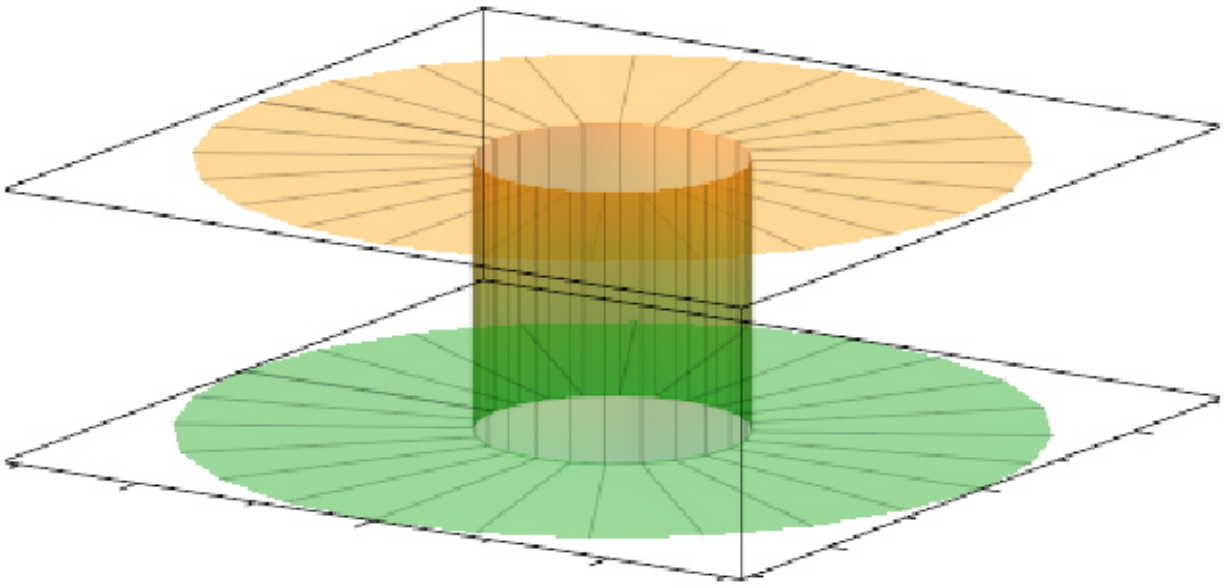

$N = 2$ wormhole geometry in the limit $n \to \infty$: A cylinder of constant radius R_0 and height $2R_0$ bridging two punctured Euclidean planes.

For these two cases the differential and integrated cross sections for plane waves incident and scattered on the upper Euclidean space are given by the following.

For $N = 2$,

$$\frac{d\sigma}{d\theta} = \frac{1}{2\pi k}\left|\sum_{m=-\infty}^{\infty}\left(S_m - 1\right)e^{im\theta}\right|^2 \ , \quad \sigma = \frac{1}{k}\sum_{m=-\infty}^{\infty}\left|S_m - 1\right|^2 \tag{57}$$

where the $N = 2$ wormhole scattering amplitudes are given by (55) with $h_{1,2} = H_m^{(1,2)}\left(kR_0\right)$ and $\kappa = \sqrt{k^2 - m^2/R_0^2}$. That is to say, no matter if $k^2R^2 \geq m^2$ so that $\kappa R = \sqrt{k^2R^2 - m^2}$ is real, or if $k^2R^2 \leq m^2$ so that $\kappa R = i\sqrt{m^2 - k^2R^2}$ is imaginary, either way $|S_m| \neq 1$. This means there is not only elastic scattering on the upper plane but also inelastic scattering, i.e. outward flux on the bottom plane.

For $N = 3$,

$$\frac{d\sigma}{d\Omega} = \frac{1}{4k^2}\left|\sum_{\ell=0}^{\infty}(2\ell+1)\,(S_\ell - 1)\,P_\ell\,(\cos\theta)\right|^2 \quad , \quad \sigma = \frac{\pi}{k^2}\sum_{\ell=0}^{\infty}(2\ell+1)\,|S_\ell - 1|^2 \tag{58}$$

where the $N = 3$ wormhole scattering amplitudes are given by (55) with $h_{1,2} = h^{(1,2)}_{\ell+1/2}\,(kR_0)$ and $\kappa = \sqrt{k^2 - \ell\,(\ell+1)\,/R_0^2}$. Again, $|S_\ell| \neq 1$. So again there is not only elastic scattering on the upper $\mathbb{E}_3$ but also inelastic scattering, i.e. outward flux on the bottom $\mathbb{E}_3$.

Here are representative s-wave ($m = 0 = \ell$) and p-wave ($m = 1 = \ell$) amplitudes for $N = 2$ and 3, plotted parametrically as functions of kR_0.

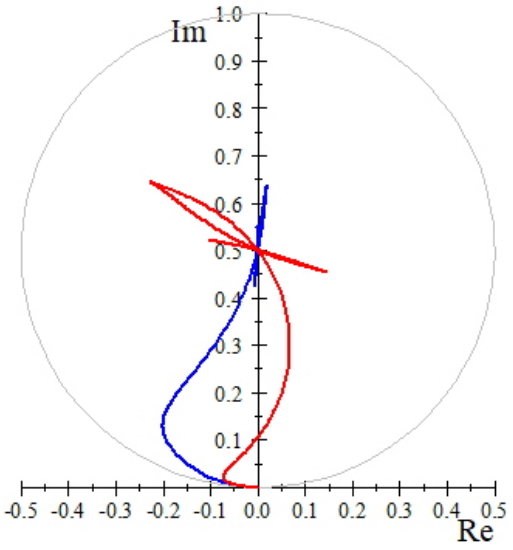

2D & 3D Wormhole $\left(\mathrm{Re}\,\frac{S_0-1}{2i}, \mathrm{Im}\,\frac{S_0-1}{2i}\right)$
for $L_0 = 2R_0$ and $0 \leq kR_0 \leq 5$, in blue & red.

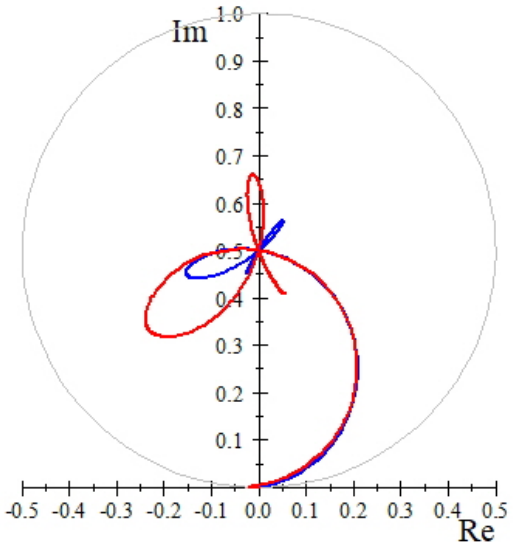

2D & 3D Wormhole $\left(\mathrm{Re}\,\frac{S_1-1}{2i}, \mathrm{Im}\,\frac{S_1-1}{2i}\right)$
for $L_0 = 2R_0$ and $0 \leq kR_0 \leq 5$, in blue & red.

Note the amplitudes lie within the unitarity circle given by $i\,(1 - \exp\,(-2ikR_0))\,/2$, thereby evincing inelastic scattering. And their asymptotic limits are the same, namely $S_{0,1} \underset{kR_0\to\infty}{\longrightarrow} 0$, albeit with non-trivial but diminishing oscillations, such that waves incident on the upper branch of the wormhole give rise to probability flux emergent only on the lower branch, in this large k limit. That is to say, for these angular momenta there are no outgoing reflected waves on the upper branch as $kR_0 \to \infty$.[2]

[2] It is noteworthy that the limiting behavior $S_\ell \underset{kR_0\to\infty}{\longrightarrow} 0$ for any fixed ℓ is what would be expected from classical trajectories for particles moving freely on the manifold. In the large momentum limit, classical particles with any fixed angular momentum will always strike and then traverse the cylinder, going from one branch of the ambient flat space to the other branch, as illustrated in the following Figure.

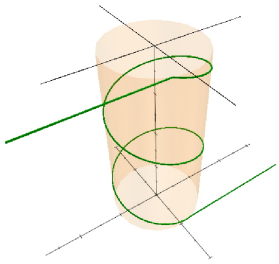

A classical trajectory, with winding number 2, for a particle transiting the $n \to \infty$ wormhole.

However, summing *all* the partial wave contributions to the integrated cross section leads to the following graphs.

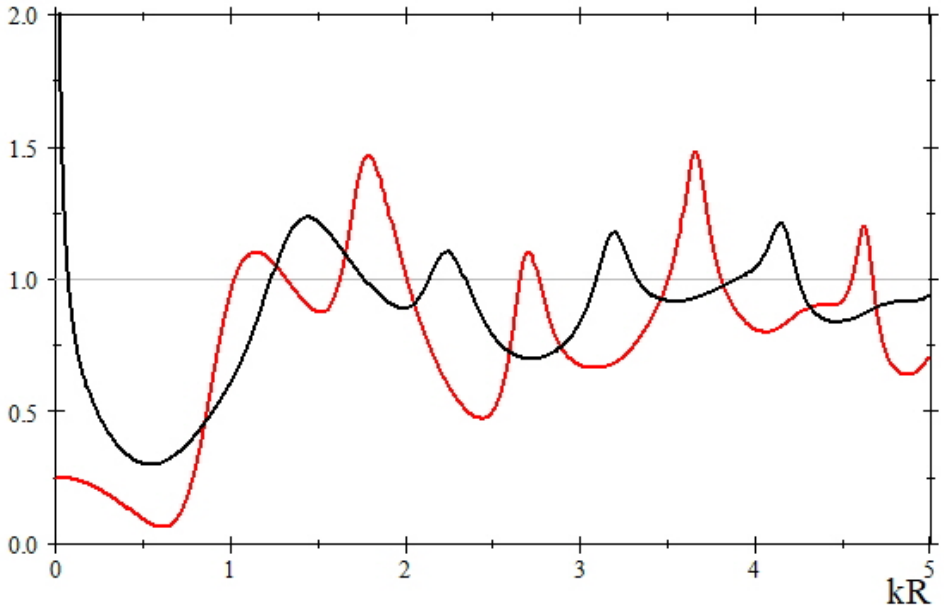

$L_0 = 2R_0$ Wormhole $\sigma/V_{N-1}\,(R)$ for $N = 2$ & 3 in black & red.

Asymptotically, for the full sum over all partial waves, $\sigma \underset{kR_0\to\infty}{\longrightarrow} 2R_0$ for $N = 2$ and $\sigma \underset{kR_0\to\infty}{\longrightarrow} \pi R_0^2$ for $N = 3$, even though any fixed angular momentum gives no contribution to σ in this limit. Note that these asymptotic results are each exactly one half of the elastic scattering cross-sections for impenetrable disk or sphere scattering, respectively.

5 Summary

The paper has exhibited various relationships between non-relativistic quantum systems involving a potential, in flat space, and systems without a potential but defined on curved manifolds. The main general results are encoded in (13), (14), (15), and (34) for N-dimensional spatial manifolds. More specific examples have been presented involving $1/r$ potentials and regularized $1/R^4$ potentials on wormhole manifolds. Perhaps our discussion should be viewed as a contemporary reconsideration of Riemann's ideas (*pre*-relativity) about universal time Newtonian dynamics in terms of geometry [16] but in the context of quantum mechanics. Or perhaps not. The reader can decide.

Acknowledgement TC thanks T. S. Van Kortryk for discussions about this work. This research was initiated when TC was the Clark Way Harrison Visiting Professor at Washington University in St. Louis.

6 Appendix: Wormhole Equatorial Slice Profiles

The following Figures show 3D embeddings for 2D equatorial slice (R, Z) profiles of various "p-norm wormholes" [14, 15] where on the equatorial plane

$$(ds)^2 = (dw)^2 + R^2(w)(d\theta)^2 = (dx)^2 + (dy)^2 + (dZ)^2 \tag{F1}$$

$$x(w,\theta) = R(w)\cos\theta\ , \quad y(w,\theta) = R(w)\sin\theta\ , \quad R(w) = \left(R_0^p + \left(w^2\right)^{p/2}\right)^{1/p} \tag{F2}$$

$$Z(w) = \int_0^w \sqrt{1 - \left(dR(\varpi)/d\varpi\right)^2}\, d\varpi = \int_0^w \sqrt{1 - (\varpi^2)^{p-1}\left(R_0^p + (\varpi^2)^{p/2}\right)^{\frac{2}{p}-2}}\, d\varpi \tag{F3}$$

For example, for $p = 2$,

$$Z(w) = R_0 \ln\left(\frac{w + \sqrt{R_0^2 + w^2}}{R_0}\right) = R_0\, \mathrm{arcsinh}\left(\frac{w}{R_0}\right) \tag{F4}$$

For generic p, it is easiest to obtain $Z(w)$ by numerical solution of

$$\frac{dZ(w)}{dw} = \sqrt{1 - (w^2)^{p-1}\left(R_0^p + (w^2)^{p/2}\right)^{\frac{2}{p}-2}} \tag{F5}$$

with initial condition $Z(0) = 0$.

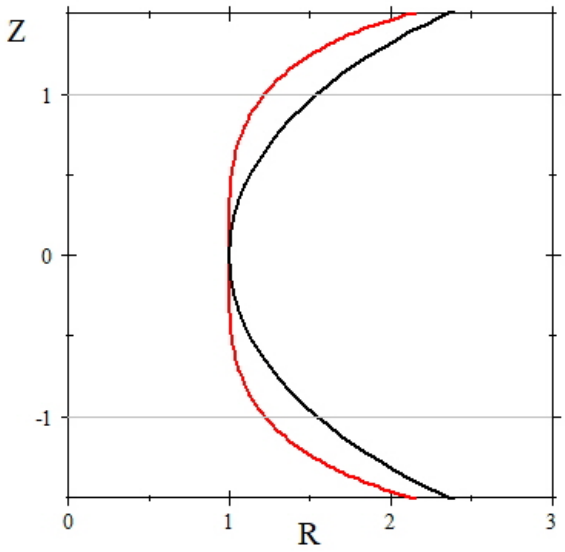

(R, Z) profile for $p = 2$ (black) compared to $p = 4$ (red).

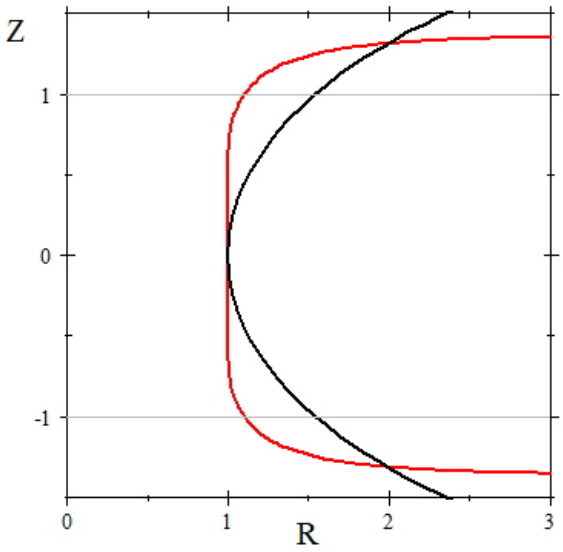

(R, Z) profile for $p = 2$ (black) compared to $p = 8$ (red).

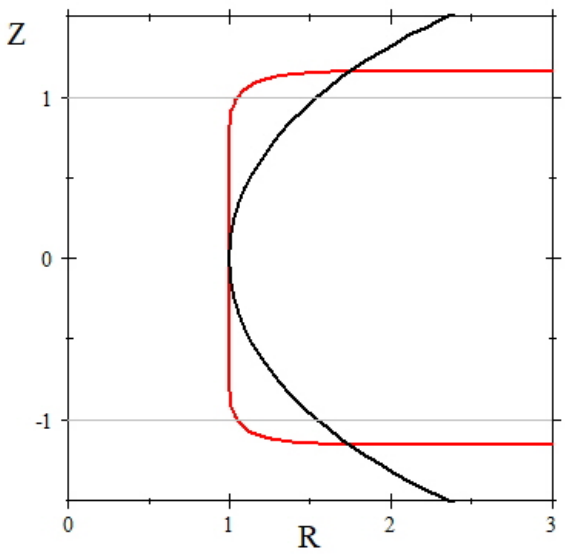

(R, Z) profile for $p = 2$ (black) compared to $p = 16$ (red).

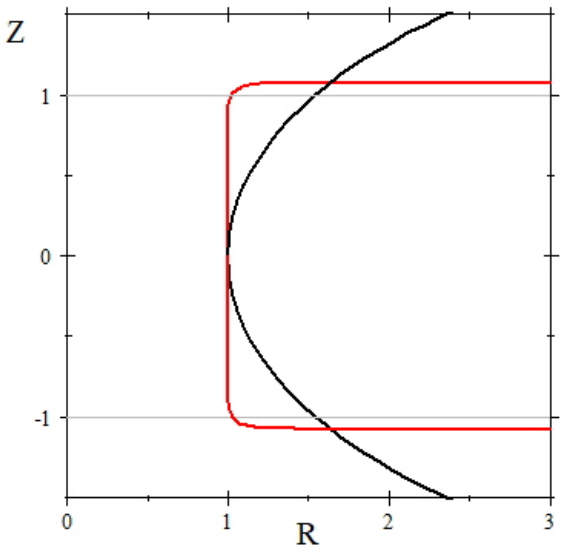

(R, Z) profile for $p = 2$ (black) compared to $p = 32$ (red).

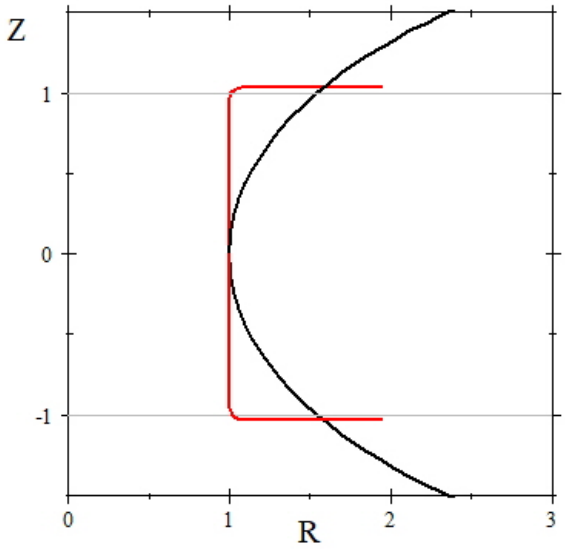

(R, Z) profile for $p = 2$ (black) compared to $p = 64$ (red).

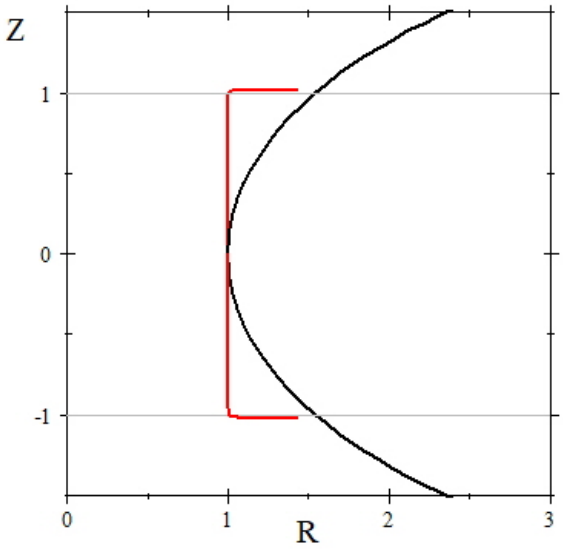

(R, Z) profile for $p = 2$ (black) compared to $p = 128$ (red).

The Figures evince the limit $p \to \infty$ very directly, for any N. In that limit the wormhole profile consists of two flat but punctured Euclidean spaces $\mathbb{E}_N$ connected by an intrinsically flat (hyper)cylinder tube whose boundaries are the (hyper)spherical holes of radius R_0 in each of the $\mathbb{E}_N$ — a manifold most easily visualized in its entirety for $N = 2$.

References

[1] C.W. Misner, K.S. Thorne, and J.A. Wheeler, *Gravitation*, Princeton University Press (2017), Chapter 25.

[2] E.L. Ince, *Ordinary Differential Equations*, Dover, New York (1956).

[3] G. Green, "Mathematical investigations concerning the laws of the equilibrium of fluids analogous to the electric fluid, with other similar researches" Trans. Cambridge Phil. Soc. 5 (1835) 1–63.

[4] A. Sommerfeld, *Partial Differential Equations in Physics*, Academic Press (1964), Appendix IV.

[5] A. Einstein and N. Rosen, "The Particle Problem in the General Theory of Relativity" Phys. Rev. 48 (1935) 73-77.

[6] M.S. Morris and K.S. Thorne, "Wormholes in spacetime and their use for interstellar travel: A tool for teaching general relativity" Am. J. Phys. 56 (1988) 395-412.

[7] H.G. Ellis, "Ether flow through a drainhole: A particle model in general relativity" J. Math. Phys. 14 (1973) 104–118.

[8] K.M. Case, "Singular Potentials" Phys. Rev. 80 (1950) 797-806.

[9] W.M. Frank, D.J. Land, and R.M. Spector, "Singular Potentials" Rev. Mod. Phys. 43 (1971) 36-98.

[10] T.L. Curtright, et al., "Charged line segments and ellipsoidal equipotentials" Eur. J. Phys. 37 (2016) 035201.

[11] H. Volkmer, Chapter 30: Spheroidal Wave Functions, NIST Digital Library of Mathematical Functions, Release 1.1.0 of 2020-12-15. F. W. J. Olver, A. B. Olde Daalhuis, D. W. Lozier, B. I. Schneider, R. F. Boisvert, C. W. Clark, B. R. Miller, B. V. Saunders, H. S. Cohl, and M. A. McClain, eds.

[12] T.L. Curtright and S. Subedi, "Holistic Scattering" *unpublished, in preparation.*

[13] T.L. Curtright and S. Subedi, "Regge Hole Theory" *unpublished, in preparation.*

[14] T. Curtright, H. Alshal, et al., "The Conducting Ring Viewed as a Wormhole" Eur. J. Phys. 40 (2019) 015206.

[15] H. Alshal and T. Curtright, "Grounded Hyperspheres as Squashed Wormholes" J. Math. Phys. 60 (2019) 032901.

[16] Riemann's pre-relativity thoughts on gravity as curved space, and related ideas by several others, are discussed here: *https://hsm.stackexchange.com/questions/9585/what-are-the-references-for-riemanns-discussion-of-gravity*

[17] K. Gottfried, *Quantum Mechanics Volume I: Fundamentals*, Chapter III, Section 15 (1966).